Low-energy nucleon-nucleon potential from Regge-pole theory

M. M. Nagels, T. A. Rijken, and J. J. de Swart
Institute for Theoretical Physics, University of Nijmegen, Nijmegen, The Netherlands
(Received 8 August 1977)

The results from a potential model for the low-energy NN interaction based on Regge-pole theory are presented. The forces are due to the dominant parts of the $\pi,\eta,\eta',\rho,\omega,\phi,\delta,\epsilon,S^*$ trajectories in the complex J plane, which are the well-known one-boson-exchange forces. Novel features are the dominant $J=0$ parts of the Pomeron, f, f', and A_2 trajectories. At the Reggeon vertices we use exponential form factors, as suggested by high-energy fits. The Pomeron, f, and f' trajectories lead essentially to repulsive central Gaussian potentials. This soft-core, partially nonlocal potential model fits the NN data with $\chi^2/\text{data} = 2.09$, which is lower than any other model we know of. The NN coupling constants have reasonable values, and the contributions of the Pomeron and tensor trajectories agree with estimates from high-energy fits.

I. INTRODUCTION

Recently we derived[1] the NN potential based on Regge-pole theory. In a dispersion-theoretic derivation of the NN potential, the new strip approximation[2] has been applied to the double-spectral functions by saturating them with t- and u-channel Regge poles. The t- and u-channel partial-wave projections of these exchanges in the Khuri-Jones representation[3] revealed that the lowest-J mesons on these trajectories dominate strongly,[1] thus leading to one-boson-exchange (OBE) potentials. Regge-pole fits at high energy suggest that the residue functions can best be parametrized with exponential forms. Whereas low-energy NN-scattering probes only a region $|t| \lesssim 0.6$ GeV^2, in high-energy scattering $|t|$ extends over several GeV^2. Therefore the behavior of the form factors at the meson vertices can be established better at high energy. We consider for the natural-parity trajectories the dominant 0^+ and 1^- mesons and for the unnatural-parity trajectories only the 0^- mesons, all with exponential form factors.

Next to the traditional boson exchanges ($\pi, \eta, \eta', \rho, \phi, \omega, \delta, \epsilon, S^*, \ldots$) we encountered some novel features: the potentials due to the Pomeron and the dominant $J=0$ contributions of the f, f', and A_2 trajectories. Because of the needed ghost-eliminating factors in the residue functions the "meson propagators" are canceled leading to Gaussian potentials. Because of the positive intercept the $I=0$ trajectories produce essentially a central repulsion, which has been estimated and which turns out to be quite strong. Therefore this may be a partial explanation for the phenomenological hard or soft cores, which one needed before.

Before we discuss the physical input we would like to stress that the present calculation is only a first step. Regge-pole theory has not been fully exploited yet. To mention a few points: the neglect of the axial-vector trajectories, no constraints from exchange degeneracy, the same effective "mass" for both the Pomeron and the f, f', A_2 contributions. We merely test in this work whether exponential form factors at the vertices and a rather strong repulsion from the diffractive and tensor trajectories can give a good quantitative description of the NN data. The $\chi^2/\text{data} = 2.09$ obtained so far shows that this is indeed the case.

We have done the calculations in configuration space and neglected all momentum dependence in the invariant potential forms except in the central potentials. These are the most important nonlocal terms. They play a crucial role in obtaining the proper shapes of the phase shifts as functions of energy. It turned out to be impossible for us to construct a soft-core one-boson-exchange or one-Reggeon-exchange potential model with only local invariant potential forms. In this respect our potential differs essentially from purely phenomenological soft-core potentials such as, e.g., the Reid potential.[11] In the latter potentials part of the soft core has to account for the momentum-dependent repulsion in the one-boson-exchange potential (OBEP) models. It is also possible to incorporate other momentum-dependent terms, but the solution of the Schrödinger equation gets more involved. We prefer to calculate in the configuration-space representation because of its high computer speed and accuracy, a powerful tool for fitting, and easy inclusion of Coulomb effects.

In this model we consider the dominant contributions of those trajectories which belong to the following mesons:

(i) The pseudoscalar mesons π, η, η'. The coupling constants are related via SU(3) and singlet-octet mixing. The value $\alpha_P = 0.361$ from the compilation of coupling constants[4] has been used for the calculation of f_{η_8}. For the singlet-octet mixing angle we use the value of the linear Gell-Mann–

Okubo mass formula $\theta_P = -23°$. The octet coupling f_π and the singlet coupling f_{η_1} are searched.

(ii) The vector mesons ρ, ϕ, ω. We assume SU(3) relations for the electric and magnetic type of couplings (see, e.g., Ref. 4, p. 86). For the electric coupling $g_V^e = g_V$ we assume $\alpha_V^e = 1$, thus coupling the ρ universally to the isospin current. The singlet-octet mixing angle is taken to be $\theta_V = 37.5°$ from the linear Gell-Mann–Okubo mass formula. The fitted coupling constants g_ρ and g_{ω_1} determine the physical coupling constants g_ρ, g_ϕ, g_ω. For the magnetic couplings $g^m = g + f$ we have no sound theoretical value for α_V^m. On the other hand, we cannot determine f_ϕ and so $g_\phi^m = (g_\phi + f_\phi)$ in the fit because of the insensitivity to variations of f_ϕ. We put $f_\phi \equiv 0$, leading to $g_\phi^m = g_\phi$. From the values of g_ρ^m, g_ϕ^m, g_ω^m we infer $\alpha_V^m = 0.449$, which is rather close to the SU(6) prediction $\alpha_V^m = 0.4$.

(iii) The scalar mesons δ, S^*, ϵ. The status of the scalar nonet is still controversial. We prefer to use the $\delta(970)$, $S^*(990)$, $\epsilon(760)$ mesons, because they fit rather nicely in the bag model[5] as crypto-exotic states. Since the singlet-octet mixing angle is still an unsettled problem,[4,6] the assumption of a value for α_S (Ref. 6) does not constrain the three couplings. Therefore all three couplings are searched.

(iv) The Pomeron P and the $J=0$ tensor contributions. In Ref. 1 we have estimated that the "effective masses" are in the range of 250 to 400 MeV depending on the various high-energy models both for the Pomeron and the tensor trajectories. For simplicity we take here a single mass parameter m_P for P, f, f', and A_2, which is a search parameter. Furthermore, we use two coupling constants: One for the total $J=0$ contribution of the $I=0$ trajectories (P, f, f'), and one for the $I=1$ contribution due to the A_2 trajectory.

Summarizing the search parameters, we fit 11 coupling constants, the Pomeron mass m_P, and the universal cutoff parameter Λ for the 0^-, 1^-, and 0^+ exchanges.

TABLE I. Values for the parameters of Eq. (23) in Ref. 7 in the two-poles approximation for the broad mesons ϵ and ρ. Masses and widths are in MeV.

	ϵ	ρ
n	0	1
m	760	770
Γ	640	146
β_1	0.18719	0.19068
m_1	500.45	647.44
β_2	0.60105	0.79649
m_2	1047.14	898.17

Finally, we mention that we treat the ρ and ϵ as broad mesons with mass distributions as given in Ref. 7. For technical reasons we can approximate the potentials by a sum of two stable mesons excellently, just as in Ref. 7. Fitting from 0.0–1.5 fm yields the values for the coefficients of Table I (for definitions see Ref. 7). The approximation to the exact forms is better than 1% everywhere.

In Sec. II we give the potentials in the momentum-space representation and in configuration space. Furthermore the solution of the Schrödinger equation with a nonlocal central potential is briefly reviewed. The results from the fit to NN are presented in Sec. III and a discussion is given in Sec. IV.

II. THE POTENTIAL MODEL

A. The potentials in momentum space

In this section we review only briefly the potentials which were obtained in Ref. 1. These are the OBE potentials with momentum-dependent central terms and exponential form factors, and the Pomeron-type potentials, where the meson (ghost) propagator has been eliminated.

Introducing the definitions

$$\vec{q} = (\vec{q}_i + \vec{q}_f)/2, \quad \vec{k} = \vec{q}_f - \vec{q}_i, \quad \vec{n} = \vec{q}_i \times \vec{q}_f = \vec{q} \times \vec{k}, \tag{1}$$

where $\vec{q}_i$ and $\vec{q}_f$ denote the initial and final three-momenta, we expand the potential[7]

$$\mathcal{V}(\vec{q}_f, \vec{q}_i) = \sum_{i=1}^{5} \mathcal{V}_i(\vec{q}_f^{\,2}, \vec{q}_i^{\,2}, \vec{q}_i \cdot \vec{q}_f) P_i . \tag{2}$$

Here the operators P_i in spin space are

$$P_1 = 1, \quad P_2 = \vec{\sigma}_1 \cdot \vec{\sigma}_2, \quad P_3 = (\vec{\sigma}_1 \cdot \vec{k})(\vec{\sigma}_2 \cdot \vec{k}), \quad P_4 = \left(\frac{i}{2}\right)(\vec{\sigma}_1 + \vec{\sigma}_2) \cdot \vec{n}, \quad P_5 = (\vec{\sigma}_1 \cdot \vec{n})(\vec{\sigma}_2 \cdot \vec{n}). \tag{3}$$

In the calculation of the invariant potential forms $\mathcal{V}_i$, we have made the following approximations for making the Fourier transformation to configuration space easier (notice that the high-$\vec{k}^2$ contributions are suppressed drastically):

(i) the energy factors

$$E = (\vec{k}^2/4 + \vec{q}^2 + M^2)^{1/2} \simeq M + \vec{k}^2/8M + \vec{q}^2/2M \tag{4}$$

(ii) we keep only terms up to first order in $\vec{k}^2/M^2$ and $\vec{q}^2/M^2$.

Using these approximations we find the $\mathcal{V}_i$ for

(i) pseudoscalar-meson exchange,

$$\mathcal{V}_3^{(P)} = -f_P^{\,2} \Delta / m_\pi^{\,2}; \tag{5}$$

(ii) vector-meson exchange,

$$\begin{aligned}
\mathcal{V}_1^{(V)} &= \{g_V^2(1-\vec{k}^2/8MM'+3\vec{q}^2/2MM') \\
&\quad - g_V f_V \vec{k}^2/[2\mathfrak{M}(MM')^{1/2}] \\
&\quad + f_V^2\vec{k}^4/(16\mathfrak{M}^2 MM')\}\Delta, \\
\mathcal{V}_2^{(V)} &= -\vec{k}^2\mathcal{V}_3^{(V)}, \\
\mathcal{V}_3^{(V)} &= \{[g_V + f_V(MM')^{1/2}/\mathfrak{M}]^2 \\
&\quad - f_V^2\vec{k}^2/8MM'\}\Delta/4MM', \\
\mathcal{V}_4^{(V)} &= -[\tfrac{3}{2}g_V^2 + 2g_V f_V(MM')^{1/2}/\mathfrak{M} \\
&\quad - 3f_V^2\vec{k}^2/8\mathfrak{M}^2]\Delta/MM', \\
\mathcal{V}_5^{(V)} &= -[g_V^2 + 8g_V f_V(MM')^{1/2}/\mathfrak{M} \\
&\quad + 8f_V^2 MM'/\mathfrak{M}^2]\Delta/16M^2M'^2;
\end{aligned} \tag{6}$$

(iii) scalar-meson exchange,

$$\begin{aligned}
\mathcal{V}_1^{(S)} &= -g_S^2(1+\vec{k}^2/8MM'-\vec{q}^2/2MM')\Delta, \\
\mathcal{V}_4^{(S)} &= -g_S^2\Delta/2MM', \\
\mathcal{V}_5^{(S)} &= g_S^2\Delta/16M^2M'^2,
\end{aligned} \tag{7}$$

where everywhere $\Delta = e^{-\vec{k}^2/\Lambda^2}/(\vec{k}^2+m^2)$; (8)

(iv) Pomeron exchange, the same as (7) but with $-g_S^2$ replaced by g_P^2 and

$$\Delta = e^{-\vec{k}^2/4m_P^2}/MM'. \tag{9}$$

In Eqs. 5–9 M and M' denote the proton and/or the neutron mass and m denotes the meson mass. The scaling mass m_π in (5) is the positive-pion mass, and the scaling mass $\mathfrak{M}$ in (6) is chosen to be the proton mass.

B. Transformation to configuration space

The method of transforming the potentials to the configuration-space representation is well known.[8] We shall only mention the Fourier transformation of the form

$$\mathcal{V}(\vec{k},\vec{q}) = \tilde{v}(\vec{k})\vec{q}^2. \tag{10}$$

One obtains for the action on the wave function

$$\langle \vec{r}|\mathcal{V}\psi\rangle = \{\tfrac{1}{4}[\nabla^2 v(\vec{r})] - \tfrac{1}{2}(\nabla^2 v(\vec{r}) + v(\vec{r})\nabla^2)\}\psi(\vec{r}), \tag{11}$$

where $v(\vec{r})$ denotes the Fourier transform of $\tilde{v}(\vec{k})$.

Next we list the Fourier transforms we need:

(i) Central potentials,

$$\int \frac{d^3k}{(2\pi)^3}\frac{e^{i\vec{k}\cdot\vec{r}}}{\vec{k}^2+m^2}(\vec{k}^2)^n e^{-\vec{k}^2/\Lambda^2} \equiv \frac{m}{4\pi}(-m^2)^n\phi_C^n(r) = (-\nabla^2)^n\frac{m}{4\pi}\phi_C^0(r). \tag{12}$$

Explicitly, we have

$$\phi_C^0(r) = \exp(m^2/\Lambda^2)\left[e^{-mr}\operatorname{erfc}\left(-\frac{\Lambda r}{2}+\frac{m}{\Lambda}\right) - e^{mr}\operatorname{erfc}\left(\frac{\Lambda r}{2}+\frac{m}{\Lambda}\right)\right]/2mr, \tag{13}$$

$$\phi_C^1(r) = \phi_C^0(r) - \frac{1}{2\sqrt{\pi}}\left(\frac{\Lambda}{m}\right)^3\exp\left[-\left(\frac{\Lambda r}{2}\right)^2\right], \tag{14}$$

$$\phi_C^2(r) = m^2\phi_C^1(r) + \frac{1}{2\sqrt{\pi}}\left(\frac{\Lambda}{m}\right)^5\left[\tfrac{3}{2}-\left(\frac{\Lambda r}{2}\right)^2\right]\exp\left[-\left(\frac{\Lambda r}{2}\right)^2\right]. \tag{15}$$

(ii) Tensor potentials,

$$\begin{aligned}
\int \frac{d^3k}{(2\pi)^3}\frac{e^{i\vec{k}\cdot\vec{r}}}{\vec{k}^2+m^2}(\vec{k}^2)^n e^{-\vec{k}^2/\Lambda^2}(\vec{\sigma}_1\cdot\vec{k})(\vec{\sigma}_2\cdot\vec{k}) &\equiv -\frac{m^3}{4\pi}(-m^2)^n[\phi_T^n(r)S_{12} + \tfrac{1}{3}\phi_C^{n+1}(r)(\vec{\sigma}_1\cdot\vec{\sigma}_2)] \\
&= -\frac{m^3}{4\pi}\{[(-\nabla^2)^n\phi_T^0(r)]S_{12} + [(-\nabla^2)^n\phi_C^1(r)]\tfrac{1}{3}(\vec{\sigma}_1\cdot\vec{\sigma}_2)\}.
\end{aligned} \tag{16}$$

The functions $\phi_T^0(r)$ and $\phi_T^1(r)$ read as follows:

$$\begin{aligned}
\phi_T^0(r) &= \frac{1}{3}\frac{1}{m^2}r\frac{\partial}{\partial r}\frac{1}{r}\frac{\partial}{\partial r}\phi_C^0(r) \\
&= \Big\{\exp(m^2/\Lambda^2)\Big[[1+mr+\tfrac{1}{3}(mr)^2]e^{-mr}\operatorname{erfc}\left(-\frac{\Lambda r}{2}+\frac{m}{\Lambda}\right) - [1-mr+\tfrac{1}{3}(mr)^2]e^{mr}\operatorname{erfc}\left(\frac{\Lambda r}{2}+\frac{m}{\Lambda}\right)\Big] \\
&\quad - \frac{4}{\sqrt{\pi}}\left(\frac{\Lambda r}{2}\right)\left[1+\tfrac{2}{3}\left(\frac{\Lambda r}{2}\right)^2\right]\exp\left[-\left(\frac{\Lambda r}{2}\right)^2\right]\Big\}\Big/2(mr)^3,
\end{aligned} \tag{17}$$

$$\phi_T^1(r) = \phi_T^0(r) - \frac{1}{6\sqrt{\pi}}\left(\frac{\Lambda}{m}\right)^5\left(\frac{\Lambda r}{2}\right)^2\exp\left[-\left(\frac{\Lambda r}{2}\right)^2\right]. \tag{18}$$

(iii) Spin-orbit potentials,

$$\int \frac{d^3k}{(2\pi)^3} e^{i\vec{k}\cdot\vec{r}} \frac{i\vec{S}\cdot(\vec{q}\times\vec{k})}{\vec{k}^2+m^2}(\vec{k}^2)^n e^{-\vec{k}^2/\Lambda^2} \equiv \frac{m^3}{4\pi}(-m^2)^n \phi_{SO}^n(r)\vec{L}\cdot\vec{S} = \frac{m^3}{4\pi}[(-\nabla^2)^n\phi_{SO}^0(r)]\vec{L}\cdot\vec{S}. \tag{19}$$

In this case we have

$$\phi_{SO}^0(r) = \frac{-1}{m^2}\frac{1}{r}\frac{\partial}{\partial r}\phi_C^0(r) = \Big\{\exp(m^2/\Lambda^2)\Big[(1+mr)e^{-mr}\operatorname{erfc}\left(-\frac{\Lambda r}{2}+\frac{m}{\Lambda}\right) - (1-mr)e^{mr}\operatorname{erfc}\left(\frac{\Lambda r}{2}+\frac{m}{\Lambda}\right)\Big] - \frac{4}{\sqrt{\pi}}\left(\frac{\Lambda r}{2}\right)\exp\left[-\left(\frac{\Lambda r}{2}\right)^2\right]\Big\}\Big/2(mr)^3, \tag{20}$$

$$\phi_{SO}^1(r) = \phi_{SO}^0(r) - \frac{1}{4\sqrt{\pi}}\left(\frac{\Lambda}{m}\right)^5 \exp\left[-\left(\frac{\Lambda r}{2}\right)^2\right]. \tag{21}$$

(iv) Quadratic spin-orbit potentials,

$$\int \frac{d^3k}{(2\pi)^3} e^{i\vec{k}\cdot\vec{r}} \frac{[\vec{\sigma}_1\cdot(\vec{q}\times\vec{k})][\vec{\sigma}_2\cdot(\vec{q}\times\vec{k})]}{\vec{k}^2+m^2} e^{-\vec{k}^2/\Lambda^2} = -\frac{m^5}{4\pi}\frac{3}{(mr)^2}\phi_T^0(r)Q_{12}+\cdots. \tag{22}$$

Only terms proportional to Q_{12} are kept. Other contributions are neglected here.

In Eqs. (13), (17), and (20) erfc denotes the complementary error function,

$$\operatorname{erfc}(x) = \frac{2}{\sqrt{\pi}}\int_x^\infty dt\, e^{-t^2}. \tag{23}$$

Note that we have defined the functions ϕ_C^n, ϕ_T^n, and ϕ_{SO}^n such that these are dimensionless and positive for large values of r.

The Fourier transforms of Pomeron-type potentials can be read off from the above formulas by the substitutions

$$\tfrac{1}{2}\Lambda \equiv m_P, \quad m=0, \quad \phi_i^{Pn} = \phi_i^{n+1}. \tag{24}$$

Explicitly we find

$$\int \frac{d^3k}{(2\pi)^3} e^{i\vec{k}\cdot\vec{r}} e^{-\vec{k}^2/4m_P^2} = \frac{1}{4\pi}\frac{4}{\sqrt{\pi}} m_P{}^3\exp(-m_P{}^2r^2), \tag{25}$$

$$\int \frac{d^3k}{(2\pi)^3} e^{i\vec{k}\cdot\vec{r}}\vec{k}^2 e^{-\vec{k}^2/4m_P^2} = \frac{1}{4\pi}\frac{8}{\sqrt{\pi}} m_P{}^5(3-2m_P{}^2r^2)\exp(-m_P{}^2r^2), \tag{26}$$

$$\int \frac{d^3k}{(2\pi)^3} e^{i\vec{k}\cdot\vec{r}} i\vec{S}\cdot(\vec{q}\times\vec{k}) e^{-\vec{k}^2/4m_P^2} = \frac{1}{4\pi}\frac{8}{\sqrt{\pi}} m_P{}^5\exp(-m_P{}^2r^2)\vec{L}\cdot\vec{S}, \tag{27}$$

$$\int \frac{d^3k}{(2\pi)^3} e^{i\vec{k}\cdot\vec{r}}[\vec{\sigma}_1\cdot(\vec{q}\times\vec{k})][\vec{\sigma}_2\cdot(\vec{q}\times\vec{k})] \simeq -\frac{1}{4\pi}\frac{16}{\sqrt{\pi}} m_P{}^7\exp(-m_P{}^2r^2)Q_{12}. \tag{28}$$

Finally, we mention the Fourier transform of the momentum-dependent central potential

$$e^{-\vec{k}^2/\Lambda^2}\vec{q}^2/(\vec{k}^2+m^2). \tag{29}$$

Using (11), we get

$$\frac{m}{4\pi}\left\{\tfrac{1}{4}m^2\phi_C^1(r) - \tfrac{1}{2}(\nabla^2\phi_C^0(r) + \phi_C^0(r)\nabla^2)\right\}. \tag{30}$$

C. The potentials in configuration space

Combining the results of the preceding subsections we end up with the following potentials in the configuration-space representation for $I=0$ exchanges.

(i) Pseudoscalar-meson exchange,

$$V_P(r) = \frac{f_P{}^2}{4\pi}\frac{m^2}{m_\pi{}^2}m[\tfrac{1}{3}(\vec{\sigma}_1\cdot\vec{\sigma}_2)\phi_C^1 + S_{12}\phi_T^0]; \tag{31}$$

(ii) Vector-meson exchange,

$$V_V(r)=\frac{m}{4\pi}\left(\left\{g_V^2\left[\phi_C^0+\frac{m^2}{2MM'}\phi_C^1-\frac{3}{4MM'}(\nabla^2\phi_C^0+\phi_C^0\nabla^2)\right]+g_Vf_V\frac{m^2}{2\mathfrak{M}(MM')^{1/2}}\phi_C^1+f_V^2\frac{m^4}{16\mathfrak{M}^2MM'}\phi_C^2\right\}\right.$$
$$+\frac{m^2}{4MM'}\left\{\left[g_V+f_V\frac{(MM')^{1/2}}{\mathfrak{M}}\right]^2\phi_C^1+f_V^2\frac{m^2}{8MM'}\phi_C^2\right\}\tfrac{2}{3}(\vec{\sigma}_1\cdot\vec{\sigma}_2)$$
$$-\frac{m^2}{4MM'}\left\{\left[g_V+f_V\frac{(MM')^{1/2}}{\mathfrak{M}}\right]^2\phi_T^0+f_V^2\frac{m^2}{8MM'}\phi_T^1\right\}S_{12}$$
$$-\frac{m^2}{MM'}\left\{\left[\tfrac{3}{2}g_V^2+2g_Vf_V\frac{(MM')^{1/2}}{\mathfrak{M}}\right]\phi_{SO}^0+\tfrac{3}{8}f_V^2\frac{m^2}{\mathfrak{M}^2}\phi_{SO}^1\right\}\vec{L}\cdot\vec{S}$$
$$\left.+\frac{m^4}{16M^2M'^2}\left[g_V^2+8g_Vf_V\frac{(MM')^{1/2}}{\mathfrak{M}}+8f_V^2\frac{MM'}{\mathfrak{M}^2}\right]\frac{3}{(mr)^2}\phi_T^0Q_{12}\right); \tag{32}$$

(iii) Scalar-meson exchange,

$$V_S(r)=-\frac{g_S^2}{4\pi}m\left[\phi_C^0-\frac{m^2}{4MM'}\phi_C^1+\frac{1}{4MM'}(\nabla^2\phi_C^0+\phi_C^0\nabla^2)+\frac{m^2}{2MM'}\phi_{SO}^0\vec{L}\cdot\vec{S}+\frac{m^4}{16M^2M'^2}\frac{3}{(mr)^2}\phi_T^0Q_{12}\right]. \tag{33}$$

(iv) Pomeron-type exchange,

$$V_P(r)=\frac{g_P^2}{4\pi}\frac{4}{\sqrt{\pi}}\frac{m_P^2}{MM'}m_P\left\{\left[1+\frac{m_P^2}{2MM'}(3-2m_P^2r^2)+\frac{m_P^2}{MM'}\vec{L}\cdot\vec{S}+\frac{m_P^4}{M^2M'^2}Q_{12}\right]\exp(-m_P^2r^2)\right.$$
$$\left.+\frac{1}{4MM'}\left[(\nabla^2\exp(-m_P^2r^2)+\exp(-m_P^2r^2)\nabla^2\right]\right\}. \tag{34}$$

For $I=1$ exchanges these potentials have to be multiplied with the operator $\vec{\tau}_1\cdot\vec{\tau}_2$ in isospin space.

D. The Schrödinger equation with a nonlocal central potential

The Schrödinger equation with a potential of the form

$$-\left[\nabla^2\frac{\phi(r)}{2M_{\rm red}}+\frac{\phi(r)}{2M_{\rm red}}\nabla^2\right] \tag{35}$$

can be solved easily by a method invented by Green.[9] Here $M_{\rm red}$ denotes the reduced mass. The radial Schrödinger equation

$$(1+2\phi)u_l''+2\phi'u_l'+[k^2-2M_{\rm red}V-(1+2\phi)l(l+1)/r^2+\phi'']u_l=0 \tag{36}$$

goes with the substitution

$$u_l=(1+2\phi)^{-1/2}v_l \tag{37}$$

formally over into the radial equation for v_l,

$$v_l''+[k^2-2M_{\rm red}W-l(l+1)/r^2]v_l=0\,. \tag{38}$$

The "potential" W in this equation is energy de-

TABLE II. Meson-nucleon coupling constants from the NN fit. As input we use f_ϕ and all masses except m_P and Λ. The underlined couplings are constrained via SU(3). Figures between parentheses give information equivalent to the ones of neighboring columns.

	m (MeV)	$g^2/4\pi$	$f^2/4\pi$	f/g
π	138.041	(13.676)	7.566×10^{-2}	
η	548.8	$\underline{(3.433)}$	$\underline{1.899}\times10^{-2}$	
η'	957.5	$\underline{(3.759)}$	$\underline{2.080}\times10^{-2}$	
ρ	770, $\Gamma=146$	0.795	14.157	(4.221)
ϕ	1019.5	$\underline{0.099}$	0	(0)
ω	783.9	$\underline{8.683}$	0.960	(0.333)
δ	962	$\underline{1.632}$		
S^*	993	0.704		
ϵ	760, $\Gamma=640$	22.731		
P,f,f'	307.81	8.778		
A_2		0.197		
Λ	964.52			

TABLE III. Nuclear-bar pp and np shifts in degrees.

T_{lab} (MeV)	25	50	95	142	210	330
$^1S_0$	49.28	39.59	26.73	16.63	5.21	−10.05
$^3S_1$	78.98	60.37	41.39	28.42	14.91	−1.84
ϵ_1	1.88	2.27	2.69	3.18	3.99	5.60
$^3P_0$	8.80	11.80	9.78	4.71	−3.45	−16.86
$^3P_1$	−4.95	−8.37	−12.87	−16.81	−21.92	−29.83
$^1P_1$	−6.04	−8.65	−11.33	−13.60	−16.63	−20.87
$^3P_2$	2.45	5.79	10.61	13.73	16.14	17.70
ϵ_2	−0.82	−1.77	−2.78	−3.11	−2.88	−1.63
$^3D_1$	−2.88	−6.61	−11.99	−16.06	−20.05	−23.60
$^3D_2$	3.92	9.77	18.99	25.57	30.35	31.13
$^1D_2$	0.67	1.63	3.50	5.47	7.94	10.51
$^3D_3$	0.08	0.47	2.00	4.15	7.32	11.43
ϵ_3	0.57	1.67	3.50	4.94	6.30	7.36
$^3F_2$	0.10	0.34	0.76	1.10	1.27	0.50
$^3F_3$	−0.23	−0.69	−1.51	−2.20	−3.02	−4.35
$^1F_3$	−0.43	−1.16	−2.18	−2.86	−3.55	−4.71
$^3F_4$	0.02	0.11	0.41	0.88	1.68	3.02
ϵ_4	−0.05	−0.19	−0.52	−0.84	−1.23	−1.74
$^3G_3$	−0.06	−0.27	−0.91	−1.75	−3.03	−5.05
$^3G_4$	0.18	0.75	2.12	3.63	5.73	8.96
$^1G_4$	0.04	0.15	0.39	0.63	1.01	1.73
$^3G_5$	−0.01	−0.05	−0.16	−0.24	−0.25	−0.04
ϵ_5	0.04	0.21	0.69	1.24	1.99	3.08
$^3H_4$	0.00	0.03	0.10	0.20	0.36	0.63
$^3H_5$	−0.01	−0.08	−0.29	−0.52	−0.85	−1.32
$^1H_5$	−0.03	−0.17	−0.52	−0.87	−1.28	−1.77
$^3H_6$	0.00	0.01	0.04	0.09	0.21	0.52
ϵ_6	−0.00	−0.03	−0.11	−0.22	−0.38	−0.64

pendent, reading

$$W=\frac{V}{1+2\phi}-\frac{1}{2M_{\text{red}}}\left(\frac{\phi'}{1+2\phi}\right)^2+\frac{2\phi}{1+2\phi}\frac{k^2}{2M_{\text{red}}}. \tag{39}$$

For $\phi>0$, which turns out to be the case here, we therefore get suppression of the wave function at small distances $r<1$ fm [$\phi(0)\simeq 1.8$ for $I=1$ and $\phi(0)\simeq 1.2$ for $I=0$]. Furthermore, we notice in (39) that for positive ϕ the energy-dependent repulsive term increases with energy.

III. RESULTS

The values of the 13 free parameters are searched in a fit to the NN data using the χ^2 second-derivative matrices of the Livermore phase-shift analysis[10] up to 330 MeV, the $^1S_0$ (pp) and $^3S_1$ (np) scattering lengths, and the deuteron parameters. The fit is very satisfactory, yielding χ^2/data = 2.09 compared to the 1128 data used in the Livermore analysis up to 330 MeV.

The obtained values for the coupling constants and searched masses are given in Table II. For $I=0$ particles we give the couplings of the physical particles, also when these result from the fitted unitary-singlet couplings, SU(3) input, and singlet-octet mixing. In Table III we have listed the resulting nuclear-bar phase shifts. The low-energy parameters for s and p waves of Eqs. (30) and (32) of Ref. 7 are given in Table IV and the deuteron parameters in Table V. Table VI displays the ^1L_L, ^3L_C, ^3L_T, and $^3L_{LS}$ phase shifts for $L=1, 2$, which are useful for low-energy analyses. Figure 1 compares the deuteron wave functions with those from the Reid soft-core potential.[11]

TABLE IV. s- and p-wave effective-range parameters in units of fm. Experimental values are taken from Ref. 4.

	a	r	a^{exp}	r^{exp}
$^1S_0$	−7.797	2.697 [a]	−7.823 ± 0.01	2.794 ± 0.015
$^3S_1$	5.468	1.818 [b]	5.424 ± 0.004	1.760 ± 0.005
$^3P_0$	−3.095	3.289	−2.6 ± 2.0	4.3 ± 2.0
$^3P_1$	1.883	−7.124	2.8 ± 1.3	−9.0 ± 1.0
$^3P_2$	−0.290	5.780	−0.45 ± 0.28	15 ± 10
$^1P_1$	2.501	−6.665		

[a] $P=0.034$.
[b] $P=-0.014$.

TABLE V. Calculated deuteron parameters. For definitions see Ref. 20.

P_d	5.39%
Q	0.2775 fm^2
$\rho(-B,-B)$	1.822 fm
N_g^2	0.8015 fm
A	0.0255

IV. DISCUSSION

A. Coupling constants

The value for $f_\pi^2/4\pi = 0.0757$ or equivalently $g_\pi^2/4\pi = 13.68$ is a little small compared to determinations of this coupling constant at the pion pole in πN scattering, where values of about 0.079 are obtained.[4] The same applies to a comparison with values from NN phase-shift analyses.[4] It is also reflected in the rather small value for the quadrupole moment of the deuteron (see below). The main reason for this rather low value is that we have approximated here $(f_\pi^2/m_\pi^2)(M/E)(\vec{\sigma}_1\cdot\vec{k})(\vec{\sigma}_2\cdot\vec{k})$ in the derivation of OPEP by $(f_\pi^2/m_\pi^2)(\vec{\sigma}_1\cdot\vec{k})(\vec{\sigma}_2\cdot\vec{k})$ in order to avoid the additional complications in the solution of the Schrödinger equation when M/E is expanded according to Eq. (4). Neglecting this effective reduction of the pion potential at higher energies has, of course, as a consequence a small reduction of the coupling constant in the fit.

For the unitary-singlet coupling $f_{\eta_1}/(4\pi)^{1/2}$ we obtain the value 0.1866. Applying the Okubo-Zweig-Iizuka (OZI) rule[12]

$$f_{\eta_1} = \sqrt{2} f_{\eta_8} \tag{40}$$

leads to 0.0997 for $f_{\eta_1}/(4\pi)^{1/2}$ from our value for f_π and the used value for α_P from Ref. 4. Therefore we have here either a considerable violation of the OZI rule or that α_P is too small. A larger value for α_P produces via the singlet-octet mixing the same physical η coupling with a smaller singlet coupling, thus reducing the violation of the OZI rule. The same happens when the π coupling is enlarged. Furthermore, the mixing angle is still a problem.

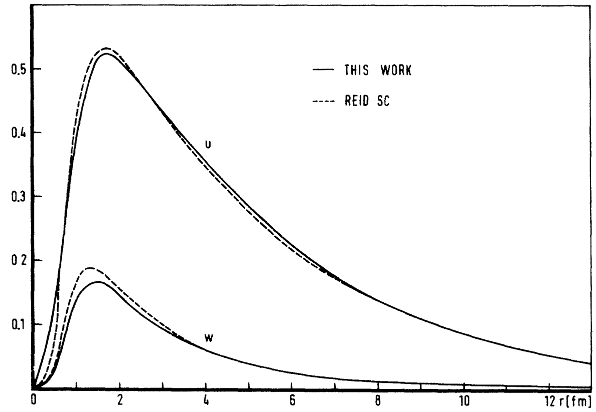

FIG. 1. The deuteron wave functions u and w. For comparison, Reid's (soft core) (Ref. 11) deuteron wave functions are also drawn.

The obtained value 3.18 for $4(g_\rho^2/4\pi)$ is a little higher than the estimated value 2.54 from $\rho\to\pi\pi$, based on the assumption of universal coupling of the ρ to the isospin current and involving an extrapolation to zero energy.[4,13] An analysis of the ρNN vertex from analytically continued πN amplitudes[14] giving, at $t=0$, $g_\rho/g_{\rho\pi\pi} = 0.52$ combined with $g_{\rho\pi\pi}^2/4\pi = 2.84 \pm 0.50$ (Ref. 4) leads to $4(g_\rho^2/4\pi) = 3.07 \pm 0.54$. The value of $f_\rho/g_\rho = 4.22$ is considerably smaller than in most NN analyses.[4,15] It is even not far away from the value 3.7 from naive ρ-meson dominance of the isovector electromagnetic form factors of the nucleon. In the aforementioned analysis of the ρNN vertex[14] one obtained at $t=0$, $f_\rho/g_\rho = 6.06$. Although a reduction of g_ρ by about 10% would improve the agreement with the ρ couplings from other determinations, the ratio f_ρ/g_ρ would still remain rather small.

A satisfactory value $g_\omega^2/4\pi = 8.68$ has been obtained in the fit. This value is considerably smaller than in most NN analyses[4,15] and implies only a small violation of the OZI rule.[12] In fact this rule yields analogously to (40) that $g_{\omega_1}/\sqrt{4\pi} = 2.18$ from g_ρ and $\alpha_V^e = 1$, whereas we have found in the

TABLE VI. Low-energy ^1L_L, ^3L_C, ^3L_T, and $^3L_{LS}$ phase shifts in degrees for $L=1,2$.

$T_{\rm lab}$ (MeV)	2	4	6	8	10	12	14
$^1P_1$	−0.481	−1.149	−1.815	−2.439	−3.013	−3.537	−4.015
^3P_C	−0.010	−0.011	0.006	0.041	0.090	0.151	0.220
^3P_T	−0.110	−0.309	−0.534	−0.766	−0.995	−1.217	−1.431
$^3P_{LS}$	0.010	0.032	0.061	0.100	0.148	0.205	0.271
$^1D_1$	0.005	0.025	0.059	0.104	0.158	0.217	0.280
^3D_C	0.005	0.023	0.056	0.100	0.154	0.216	0.284
^3D_T	0.013	0.062	0.143	0.251	0.378	0.522	0.677
$^3D_{LS}$	0.001	0.006	0.013	0.021	0.031	0.041	0.051

fit $g_{\omega_1}/\sqrt{4\pi}=2.53$. This rather small value is clearly a consequence of the inclusion of the repulsive Pomeron and $J=0$ contributions of the f and f' trajectories. The physical coupling $g_\phi^2/4\pi=0.10$, which is a consequence of the SU(3) constraints, is close to zero. From the magnetic couplings g_ρ^m, g_ϕ^m, and g_ω^m we infer $\alpha_V^m=0.449$, which is close to the SU(6) prediction $\alpha_V^m=0.4$. In this case the OZI rule predicts $g_{\omega_1}^m/\sqrt{4\pi}=3.03$ using g_ρ^m and α_V^m, whereas we have $g_{\omega_1}^m/\sqrt{4\pi}=3.31$, again only a small violation. We notice that $f_\omega/g_\omega=0.33$ is quite different from zero, in contrast to what many authors claim from naive vector-meson dominance of the isoscalar electromagnetic formfactors of the nucleon. We would like to stress here that it is impossible to determine g_ω or f_ω in an analysis of the electromagnetic formfactors. The photon belongs to an octet. Therefore the singlet part of the ω enters only in the SU(3)-breaking part. In exact SU(3) symmetry it would decouple completely. So claims about g_ω or f_ω are in fact claims about the breaking of SU(3). Furthermore, the ψ meson contributes essentially to the isoscalar electromagnetic current.[16]

There exists little information about the couplings of the scalar mesons. The values for g_ϵ seem to be widely spread.[4,15] However, this is essentially a consequence of the different treatments of the broad-meson problem. Our value $g_\epsilon^2/4\pi=22.73$ is about 10% lower than in earlier hard-core models.[4,7]

For the mass parameter in the Pomeron-type potentials we estimated in Ref. 1 from the Regge-pole model of Ref. 17 for $m_P=250$ MeV and $m_{P'}=240$ MeV. A more recent fit[18] leads to $m_P=290$ MeV and $m_{P'-\omega}=360$ MeV, the latter one representing an effective trajectory. The searched value $m_P=307.8$ MeV agrees well with these estimates. As to the couplings we note that the $I=0$ contribution is much larger than the $I=1$ contribution. This is consistent with high-energy fits, where it is well known that the A_2 trajectory couples much weaker than the P, f, f' trajectories. For the strength of the total $I=0$ potential we have estimated in Ref. 1 from the results of Ref. 17 that the central potential at $r=0$ is about 600 MeV. From our fitted values we arrive at

$$V_C^{P,f,f'}(r=0)=655\text{ MeV}, \tag{41}$$

indicating that the coupling constants we found have the correct order of magnitude.

B. Phase shifts and low-energy parameters

The $^3D_2$ phase shift poses a serious problem in most of the theoretical models by growing too large at high energies. The present model having a phase shift $\delta=31.13°$ at $T_{\text{lab}}=330$ MeV is already quite reasonable. Inclusion of the momentum-dependent terms in the pion potential, which we have neglected here, depresses the phase shift to about 27° at $T_{\text{lab}}=330$ MeV. Therefore we conclude that the inclusion of the Pomeron-type potentıa's helps to solve the problem in the $^3D_2$ wave.

With respect to the scattering lengths and effective ranges (Table IV) we mention that we have fixed the binding energy of the deuteron at its experimental value. This way the $^3S_1$ scattering length deviates a little from its experimental value. However, a more refined treatment is necessary[19] for getting all low-energy parameters in the different charge modes consistent with experiment. The rather low value of the quadrupole moment Q of the deuteron is a consequence of the low pion coupling, which essentially determines Q. A coupling of about $f_\pi^2/4\pi=0.0785$ or $g_\pi^2/4\pi=14.2$ is necessary to bring Q to its experimental value.[4] We note that although our value for Q is close to the one from Reid's soft-core potential[11] the d-state probability is considerably lower in our model. The low-energy parameters for the p waves resemble very much those from the hard-core models.[4,7]

[1] T. A. Rijken, in *Proceedings of the International Conference on Few Body Problems in Nuclear and Particle Physics, Quebec, 1974*, edited by R. J. Slobodrian, B. Cuec, and R. Ramavataram (Presses Univ. Laval, Quebec, 1975), p. 136; T. A. Rijken, Ph.D. thesis, University of Nijmegen, 1975 (unpublished); T. A. Rijken and M. M. Nagels (unpublished).

[2] G. F. Chew and C. E. Jones, Phys. Rev. 135, B208 (1964); G. F. Chew, *The Analytic S-Matrix* (Benjamin, New York, 1966).

[3] C. E. Jones, Lawrence Rad. Lab. Report No. UCRL-10700, 1962 (unpublished); N. N. Khuri, Phys. Rev. 130, 429 (1963).

[4] M. M. Nagels *et al.*, Nucl. Phys. B109, 1 (1976).

[5] R. L. Jaffe, Phys. Rev. D 15, 267 (1977).

[6] M. M. Nagels, T. A. Rijken, and J. J. de Swart, University of Nijmegen, Report No. THEF-NYM-77.8, 1977 (unpublished).

[7] M. M. Nagels, T. A. Rijken, and J. J. de Swart, Phys. Rev. D 12, 744 (1975); 15, 2547 (1977).

[8] N. Hoshizaki and S. Machida, Prog. Theor. Phys. 24, 1325 (1960).

[9] A. M. Green, Nucl. Phys. 33, 218 (1963).

[10] M. H. MacGregor, R. A. Arndt, and R. M. Wright, Phys. Rev. 182, 1714 (1969).

[11] R. V. Reid, Ann. Phys. (N.Y.) 50, 411 (1968).

[12] S. Okubo, Phys. Lett. 5, 165 (1963); G. Zweig, CERN Report No. 8419/TH 142, 1964 (unpublished); J. Iizuka, K. Okada, and O. Shito, Prog. Theor. Phys. 35, 1061 (1966).

[13]F. M. Renard, Nucl. Phys. B15, 267 (1970).
[14]G. Höhler and E. Pietarinen, Nucl. Phys. B95, 210 (1975).
[15]J. J. de Swart and M. M. Nagels, University of Nijmegen, Report No. THEF-NYM-77.4, 1977 (to be published in Fortschr. Phys.).
[16]D. Cords and G. Weber, DESY Report No. 77/21, 1977 (unpublished).
[17]W. Rarita, R. J. Riddell, C. B. Chiu, and R. J. N. Phillips, Phys. Rev. 165, 1615 (1968).
[18]P. D. B. Collins, F. D. Gault, and A. Martin, Phys. Lett. 47B, 171 (1973).
[19]G. J. M. Austen (private communication).
[20]L. Hulthén and M. Sugarawa, in *Handbuch der Physik*, edited by S. Flügge (Springer, Berlin, 1957), Vol. 39, p. 1.